Visualizations for Diagnosing Network Models

Sam Tyner

Department of Statistics and Statistical Laboratory, Iowa State University

and

Heike Hofmann

Department of Statistics and Statistical Laboratory, Iowa State University

July 10, 2019

Abstract

Statistical models for networks have been studied for decades, and they have gotten more complex as computing power has grown. Some network models, such as those for dynamic social networks, are analytically intractable and therefore require extensive simulation procedures for model fitting. In this paper, we use model visualization techniques to better understand some of these models and their behavior. We use a three-pronged visualization attack: (a) network visualizations to view the model, (b) visualizations of collections of models to interpret parameters, and (c) visualizations of fitting algorithms to gain insights into the underlying mechanisms. With the help of static and dynamic visualizations, we bring the hidden algorithmic fitting processes into the foreground, with the goal of a better understanding and higher accessibility of statistical models for social network analysts.

Keywords: social network analysis, dynamic networks, network mapping, animation, statistical graphics

Contents

1   Introduction & Background

Scholars have been trying to understand relationships between people, or *social networks*, for decades, especially in the social sciences. There are a host of quantitative methods available for analyzing social networks, including statistical models, such as exponential random graph models (ERGM) and latent space models (LSM), that strive to capture the underlying network-generating mechanism (Frank and Strauss, 1986; Hoff et al., 2002). The ERGM and LSM families are examples of static network models, which focus on a single "snapshot" of a network and "global network statistics" such as outdegree distribution (Goldenberg et al., 2010). Other static network model families include the Erdös-Rényi random graph model and the exchangeable graph model (Goldenberg et al., 2010). These static models, however, are not optimal for modeling real networks because they do not account for changes in the network as time passes. In real networks, edges may be created or destroyed, and nodes can be born or die (Goldenberg et al., 2010). Dynamic models for networks, which model networks observed at many points in time, are the more realistic alternative to static network models.

Dynamic network models do not have as rich of a history as static network models, largely due to the historical lack of data and available analytical tools (Goldenberg et al., 2010). With the advent of social media and ever-increasing computational power, however, more and more researchers are turning their attention toward dynamic network models. Some of the classical models, such as the Erdös-Rényi model and the small-world model of Watts and Strogatz (1998) are pseudo-dynamic because they could be applied in a dynamic way but rarely are (Goldenberg et al., 2010). Fully dynamic social network models, however, are more complicated: they incorporate both the network structure and its changes in time. If we can capture this change mechanism in time, we can truly begin to model the underlying network dynamics that drive social connections. A comprehensive review of dynamic network models is presented in Goldenberg et al. (2010).

We are particularly interested one truly dynamic family of network models: continuous time Markov chain (CTMC) models, first introduced in Holland and Leinhardt (1977). We chose these models because they correspond to our intuition about how social networks are formed, and they are very flexible and widely applicable. In these models, network changes

are modeled hierarchically at the node level: nodes are given opportunities to change via a rate function, then the node chooses which edge to change according to its utility function. In each step of the hierarchy, many possible effects can be implemented to capture the change mechanism. For example, the rate function could be a simple waiting-time model, or it could depend on a node's indegree or outdegree: we may have reason to believe that the more popular nodes change their ties more frequently. In addition, we can incorporate node covariate information into the hierarchy, such as gender or education level of people in a social network. For instance, the genders of two people could effect whether and how quickly they establish a relationship, and people will likely form more relationships with those who share their education level. Thus, the transition probabilities between two states of a network depend on the network's structure, characteristics of the nodes, or both (Snijders, 1996). For example, Schaefer et al. (2011) use a CTMC model to learn about the tendency of depressed adolescents to form friendships and found that depressed students tended to avoid creating new friendships over time. The CTMC model family can also be expanded to model node behavior, as in Chyzh (2016), who applies CTMC models to show that more indirect trade relationships in a country decrease its overall respect for human rights. Thus, with CTMC models we can examine assumptions made about social networks.

With the flexibility of CTMC models comes increased complexity and estimation difficulty (Snijders, 2017). Likelihood functions quickly become very complex due to the inherent dependency structure in the data, and therefore computational methods, such as Markov chain Monte Carlo (MCMC), are used to fit models. Methods for maximum likelihood estimation (MLE) for these models were not introduced until Snijders et al. (2010b), and method of moments (MM) estimation is frequently used (Ripley et al., 2016). For CTMC parameter estimation, we use the software SIENA, and its `R` implementation `RSiena` (R Core Team, 2016; Ripley et al., 2016). This software is a considerable contribution to the field of social network analysis, allowing for estimation of structural effects, node covariate effects, as well as modeling both network and node changes in a wide variety of CTMC models. This extensive parameter estimation process is largely hidden from the user, and the primary outputs are parameter estimates. Direct simulation from a given

4

network model with fixed parameter values is also made easy with `RSiena`. This software opens up a great deal of possibilities for network modeling and simulation.

Since we chose the CTMC models for dynamic social networks, we would like to determine how well they fit data. We chose these models because they match our intuition about how social networks form in reality, and after we fit a model, we will want to assess its goodness-of-fit. In statistical network models generally, the lack of large-sample theory leads to a lack of goodness-of-fit tests (Goldenberg et al., 2010). Most methods for assessing goodness-of-fit for network models, therefore, involve comparing statistics computed on simulated networks to the same statistics computed on the data, for example in Hunter et al. (2008a). More recently, Schweinberger (2012) used score-type tests for forward model selection in the CTMC model context. The `RSiena` software also contains methods for goodness-of-fit based on network statistics, such as outdegree distribution, where the data values are compared to simulated values as in Hunter et al. (2008a) (Ripley et al., 2016).

We propose new methods for goodness-of-fit and other diagnostics that use visualization as a supplement to computational methods. Network visualization, also called graph drawing, is a prominent subfield of network analysis with a rich history: early drawings of complete graphs date back to 1280 CE (Knuth, 2013). We use this visualization foundation to combine modeling with visualization. Note that we do not propose new methods of visualizing networks, and for a complete review of the field of graph drawing we direct the reader to Tamassia (2013). What is novel in our work is the use of common visualization methods to diagnose network model with model visualization

Model visualization complements traditional model diagnostic tools such as R^2 values and residual plots to enrich our understanding and interpretation of statistical models (Wickham et al., 2015). We apply the three principles of model-vis: view the model in the data space, visualize collections of models, and explore the process of fitting the model, to the models and data introduced in Section 2. By translating the model visualization work of Wickham et al. (2015) to the dynamic network model space, we provide network researchers with a new suite of tools for visualizing and diagnosing performance of their network models. Though we apply the tools to CTMCs because we find the models intuitive, the methods

we use can be applied to any network model, static or dynamic.

In the remainder of this section, we provide an overview of the structure of network data and discuss two common network visualization (net-vis) techniques. Then, we detail the hierarchical model structure of a CTMC following the definition in Snijders (1996) and ouline the CTMC model fitting process in `RSiena` (Snijders, 2016).

1.1   Networks and their Visualizations

Network data across fields have similar structure: they consist of units of observation and connections between those units. In a social network, the units of observations, called *nodes* or *actors*, are people, while the connections, called *edges* or *ties*, are their relationships with each other. Other network data include inherent variables of interest on the nodes, such as age or gender, and the type of relationship (friends, coworkers, etc) that an edge represents. Dynamic networks are observed at many discrete points in time, where each observation of a network is often called a "wave" of data.

Visualizing Network Data: Visualizing network data is inherently challenging due to the structure of the data itself. Most data visualizations rely on well-defined axes inherited from the data, such as Cartesian coordinates or spatial locations, but network data typically do not have such built-in structure.
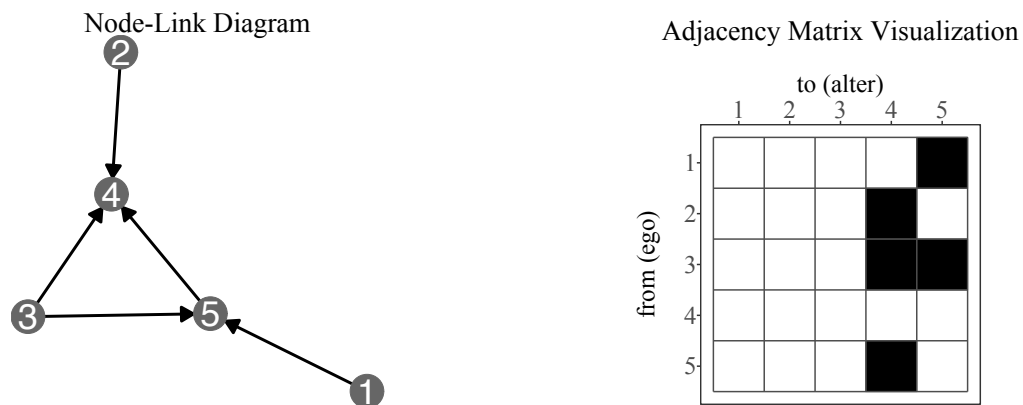

Figure 1: On the left, a node-link diagram of our toy network, with nodes placed using the Kamada-Kawai algorithm. On the right, the corresponding adjacency matrix visualization.

The lack of a native coordinate system has given rise two primary net-vis methods: the node-link diagram and the adjacency matrix visualization (Fekete, 2009). We demonstrate

these with a simpe example. Consider the network with five nodes, $\{1, 2, 3, 4, 5\}$, connected by five directed edges: $\{2 \to 4, 3 \to 4, 1 \to 5, 3 \to 5, 5 \to 4\}$ shown in Figure 1.

The first net-vis method, the node-link diagram, represents nodes with points in two dimensions and then represents edges by connecting the points with lines. These lines can also have arrows on them indicating the direction of the edge for directed networks, as shown in Figure 1. Because there is often no natural placement of the nodes, they are placed in 2D at random, then adjusted with a layout algorithm. Some commonly used algorithms, such as the Kamada-Kawai (KK) layout (Kamada and Kawai, 1989) and the Fruchterman-Reingold (FR) layout (Fruchterman and Reingold, 1991), are designed to mimic physical systems, drawing the graphs based on the "forces" connecting them. For a full discussion of available node-link layout algorithms, we direct the reader to Gibson et al. (2013). In Figure 1, we use the KK algorithm, and unless otherwise stated, all other node-link diagrams in this paper are laid out using the KK algorithm (Kamada and Kawai, 1989).

The second method for net-vis uses the adjacency matrix of the network. The adjaceny matrix of a network, $\mathbf{A}(x)$ is defined as:

$$A_{ij}(x) = \begin{cases} 1 & \text{if } x_{ij} = 1, \quad i \neq j \\ 0 & \text{otherwise} \end{cases} \tag{1}$$

The adjacency matrix visualization for our toy example is also shown in Figure 1. This visualization shows the network as a grid, with each row representing the "from" or "ego" node and each column representing the "to" or "alter" node of an edge. The grid space for x_{ij} (the edge $i \to j$) is filled in if $A_{ij} = 1$ and is empty if $A_{ij} = 0$. For undirected networks $\mathbf{A}$ is symmetric, so the adjacency matrix visualization is also symmetric, with each edge drawn twice.

Each net-vis method has its own advantages and disadvantages. For instance, paths between two nodes in a network are easier to determine with node-link diagrams than with adjacency matrix visualizations (Ghoniem et al., 2005). Furthermore, in node-link diagrams, node information can be incorporated into the visualization by coloring or changing the shape of the points, and edge-level information can be incorporated by coloring the lines or changing their thickness. Visualizing a node variable in an adjacency matrix vi-

sualization is not as simple, because this type of net-vis features the edges. An adjacency matrix visualization can, however, be useful when the network is very complex, dense, or large (Ghoniem et al., 2005). Ultimately, there is no one "correct" way to visualize network information, and we will be using both the node-link and adjacency matrix net-vis methods throughout this paper to visualize our example data and CTMC models.

1.2   Defining CTMC Network Models

The continuous-time Markov chain (CTMC) model family is for analyzing dynamic networks, so we can use them to study the change of a network in time while also examining the structural and node covariate efects. To define CTMCs for our purposes, we follow the general hierarchical definition outlined in Snijders (2017) and elsewhere (see e.g. Snijders (2001) and Snijders et al. (2010a)). CTMC models reflect our intution about social networks: most social networks, even holding constant the set of actors over time, are ever-changing as relationships form or dissolve. Actors in social networks also have properties that could change their role within the network, and existing ties may affect formation or dissolution of other ties. In this section, we define the data structure, the hierarchal model, and intensity matrix of the CTMC.

1.2.1   Definitions, Terminology, and Notation

A dynamic network consists of a fixed set of n nodes that is changing over time, and is observed at M discrete time points, $t_1, \ldots, t_M$ with $t_1 < t_2 < \cdots < t_M$. We denote the network observation at timepoint t_m by $x(t_m)$ for $m = 1, \ldots M$. The model assumes that this longitudinal network of discrete observations is embedded within a CTMC, which we denote by $X(T)$. The CTMC is almost entirely unobserved: we assume the first and last network observations are the starting and ending points of the CTMC, i.e. $x(t_1) \equiv X(0)$ and $x(t_M) \equiv X(\infty)$. Nearly all other steps in the chain are unobserved, with the exception of $x(t_2), \ldots, x(t_{M-1})$. Unlike the first and last observations of the network, $x(t_2), \ldots, x(t_{M-1})$ do not have direct correspondence with steps in the CTMC. Thus, the observations $x(t_2), \ldots, x(t_{M-1})$ treated as "snapshots" of the network at some point between two steps in the CTMC.

The CTMC process $X(T)$ is a series of single tie changes that happen according to the model's *rate function*, the first piece of the hierarchy. One actor at a time is "selected" to make a change, then in the second piece of the hierarchy, it randomly changes its ties according to probabilities derived from the *objective function*.

Rate Function: In general, the *rate function*, $\rho(x, \mathbf{Z}, \boldsymbol{\alpha})$, is a function of the network at its current state x, covariates of interest, $\mathbf{Z}$, and some parameters, $\boldsymbol{\alpha}$. With this general formulation, each node can have a different rate of change. Throughout this paper, we assume a simple rate function, $\rho(x, \mathbf{Z}, \boldsymbol{\alpha}) \equiv \alpha_m$ that is constant across all actors between time t_m and t_{m+1}. With this simple rate function, we have $M - 1$ rate parameters, one for each transition from $x(t_m)$ to $x(t_{m+1})$ for $m = 1, \ldots, M - 1$. The rate parameter, α_m dictates how often an actor i is selected to change one of its ties, x_{ij}, for $j \neq i \in \{1, \ldots, n\}$ in the time period from t_m to t_{m+1} for $m = 1, \ldots, M - 1$. The CTMC model assumes that the actors i are conditionally independent given their ties $x_{i1}, \ldots, x_{in}$ at the current network state. Let $\tau(i|x, m)$ be the wait time until actor i gets to the opportunity to change its ties. For any time point T, where $t_m \leq T < t_{m+1}$, the waiting time to actor i's next change follows an exponential distribution,

$$\tau(i|x_{i1}(m), \ldots, x_{in}(m)) \overset{\text{iid}}{\sim} Exp(\alpha_m) \tag{2}$$

with expected value α_m^{-1}. From Equation 2, we can derive the waiting time to the next change opportunity by *any* actor in the network, $\tau(x)$. The value $\tau(x)$ is also exponentially distributed, and has expected value $(n\alpha_m)^{-1}$. The estimation of α_m in `RSiena` is simple: method of moments (MoM) is used with the statistic

$$C_m = \sum_i \sum_j |x_{ij}(t_{m+1}) - x_{ij}(t_m)|, \tag{3}$$

which is the total number of edge differences between $x(t_m)$ and $x(t_{m+1})$.

Objective Function: Because of the conditional independence assumptions given in Equation 2, the objective function can be written separately for each node. Suppose node i is selected to change at the next step in the CTMC. This node, called the *ego* node, has the potential to interact with all other nodes in the network, $j \neq i$. These nodes j, are referred to as *alter* nodes, and will not change any of their ties at the next step in the CTMC. The

ego node i in the current network state x, prioritizes making changes that maximize its *objective function*:

$$f_i(\boldsymbol{\beta}, x, \mathbf{Z}) = \sum_{k=1}^{K} \beta_k s_{ik}(x, \mathbf{Z}), \tag{4}$$

where x is the current network state, $\mathbf{Z}$ is a matrix of node covariates, and K is the total number of parameters in the objective function. The parameters of the model, $\beta_1, \ldots, \beta_K$ correspond to network statistics, $s_{ik}(x, \mathbf{Z})$, for $k = 1, \ldots, K$. To maximize f_i, i will either destroy a tie, create a tie, or make no change.

The parameters of $f_i(\boldsymbol{\beta}, x, \mathbf{Z})$ are either structure or covariate parameters. The structure parameters correspond to statistics that are *only* functions of the current network state, x, while the covariate parameters are also functions of the covariates, $\mathbf{Z}$. According to Snijders (2001, p. 371), there should be at least two parameters in the objective function: β_1 for the outdegree of nodes, and β_2 for the reciprocity of nodes. The former measures the propensity of nodes with a lot of outgoing ties to form more outgoing ties (the "rich get richer" effect), while the latter measures the tendency of outgoing ties to be returned within a network. The statistics corresponding to these two parameters, $s_{i1}(x)$ and $s_{i2}(x)$ are given in Figure 3 with visualizations of the corresponding effects. In the RSiena software, there are over 80 possible $\boldsymbol{\beta}$ parameters with corresponding statistics $s_{ik}(x, \mathbf{Z})$ to add to the model. The definition of the statistics for all possible parameters are provided in Ripley et al. (2017), and two additional parameters and their corresponding statistics are discussed in Section 2 and shown in Figure 3.

In the CTMC, when actor i can make a change, it chooses which tie $x_{i1}, \ldots, x_{in}$ to change at random according to the probability $p_{ij}(\boldsymbol{\beta}, x, \mathbf{Z})$. Let $x(i \rightsquigarrow j)$ be the network identical to network x with the exception of tie x_{ij}, which is equal to $1 - x_{ij}$; i.e. the presence or absence of node x_{ij} is flipped in the new network. The probability that the tie x_{ij} changes is defined as:

$$p_{ij}(\boldsymbol{\beta}, x, \mathbf{Z}) = \frac{\exp\left\{f_i(\boldsymbol{\beta}, x(i \rightsquigarrow j), \mathbf{Z})\right\}}{\sum_{h \neq i} \exp\left\{f_i(\boldsymbol{\beta}, x(i \rightsquigarrow h), \mathbf{Z})\right\}} \tag{5}$$

We explore these probabilities further in Section 5.

Intensity Matrix: The probabilities p_{ij} combined with the rate parameters α_m fully characterize the underlying CTMC that models network change. In the CTMC literature,

10

see for instance Yin and Zhang (2010), chains are characterized by their *intensity matrix* $\mathbf{Q}$. This matrix describes the rate of change between two states of the CTMC process, and the rows of this matrix always add to zero. The state space for a network, denoted $\mathcal{X}$, contains $2^{n(n-1)}$ states: there are two possible states for an edge, $\{0, 1\}$, and $n(n-1)$ possible edge relationships, as the network is directed and we exclude self-ties. The intensity matrix is then a square matrix of dimension $2^{n(n-1)}$. Only one tie changes at a time in the CTMC, resulting in $n(n-1)$ reachable states from the current network state. Thus, the intensity matrix $\mathbf{Q}$ is very sparse, with only $n(n-1) + 1$ non-zero entries in each row. Note that $n(n-1)$ of these entries represent the possible states that are one edge different from a given state, while the additional non-zero entry is the diagonal entry for the current state.

The two pieces of the model hierarchy each contribute to the intensity matrix to describe the rate of change between two network states. The entries of $\mathbf{Q}$ are defined as follows: let $b \neq c \in \{1, 2, \ldots, 2^{n(n-1)}\}$ be indices of two different possible states of the network, $x^b, x^c \in \mathcal{X}$. Then the bc^{th} entry of $\mathbf{Q}$ is:

$$
q_{bc} = \begin{cases} q_{ij} = \alpha_m p_{ij}(\boldsymbol{\beta}, x^b) & \text{if } x_{ij}^c = 1 - x_{ij}^b \text{ for some } i \neq j \in \{1, 2, \ldots, n\} \\ -\sum_{i \neq j} q_{ij} & \text{if } x^b = x^c \\ 0 & \text{otherwise} \end{cases}
$$

Thus, the rate of change between any two states, x^b and x^c, that differ by only one tie x_{ij}, is the product of the rate at which actor i gets to change a tie and the probability that the tie that will change is the tie to node j. The intensity matrix $\mathbf{Q}$ fully defines the CTMC model for network change.

1.2.2 Fitting Models to Data

To fit a CTMC to dynamic network data, we apply the `RSiena` software, which uses simulation methods to estimate parameter values using either MoM or maximum likelihood (ML) estimation (Ripley et al., 2016). We chose to use MoM estimation, so we describe that process here, while more information on ML estimation can be found in Snijders (2016). The underlying SIENA software uses a Robbins-Monro algorithm (see Robbins and Monro

(1951)) to estimate the solution of the moment equation

$$E_\theta S = s_{obs} \qquad (6)$$

where $\theta = (\boldsymbol{\alpha}, \boldsymbol{\beta})$ is the vector of rate and objective function parameters, and s_{obs} is the observed vector of the corresponding statistics summed over all network observations. Estimation conditions on the first observed network, $x(t_1)$, then proceeds to estimate model parameters for all future observations. The full SIENA MoM estimation algorithm operates in three phases, as described in Ripley et al. (2017) and Snijders (2016), which we briefly summarize here. The first phase obtains initial estimates of the score functions for use in the second phase. The second phase is the Robbins-Monro algorithm, and results in parameter estimates through iterative updates and simulation from the CTMC at the iterations of the parameter values. The third phase uses the parameters from phase two to estimate the score functions and covariance matrix of the parameter estimates and carries out convergence checks. In Section 5, we further explore these phases in the SIENA MoM algorithm through visualization. For a more detailed description of the fitting process, we direct the reader to Ripley et al. (2017); Snijders (2016)

The rest of this paper is strucured as follows. In Section 2, we introduce the motivating data and CTMC models we assess using model-vis. Then, in Section 3, we explore the first step in model-vis by placing the models in the data space to determine how well the models fit the data. Section 4 follows, in which we visualize collections of models to explore their behavior. Finally, in Section 5, we visualize the underlying algorithms in the CTMC fitting process to gain insight into the fitting process. We conclude with a discussion in Section 6.

2   Example Data and Models

Example Data: To guide our visual exploration of CTMC models for dynamic networks, we use a canonical example in the social network literature: a subset of the 50 actor dataset from the "Teenage Friends and Lifestyle Study" Michell and Amos (1997). We chose this data because it is a well-known and easy to understand example. We were all teenagers once, and we know the volatility and fragility of those relationships, as well as why they might change. We chose to only work with a subset of the data to make node-link diagrams
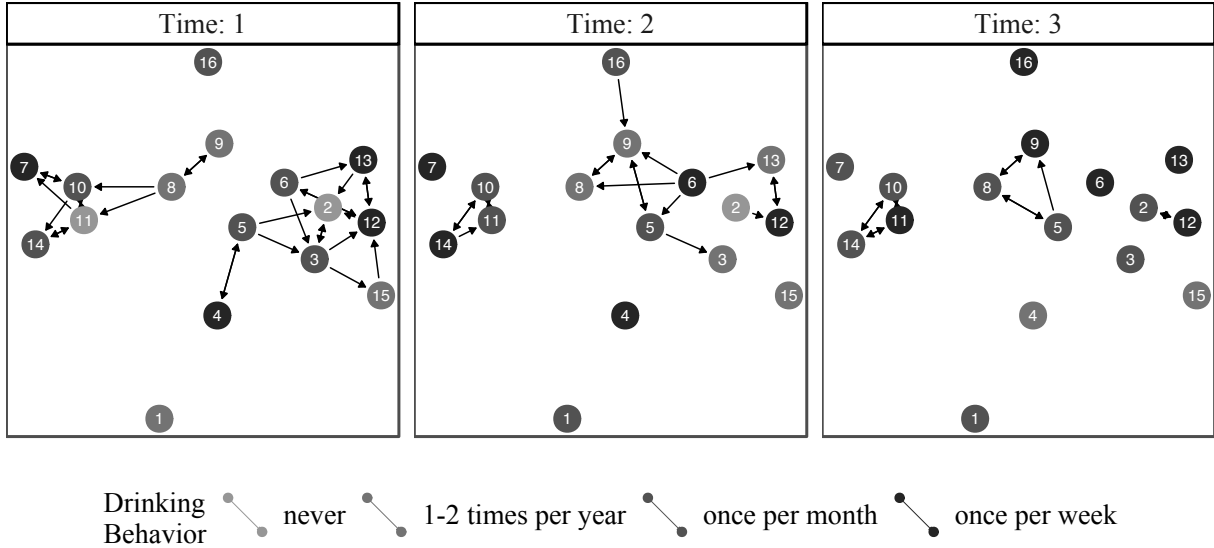
Figure 2: The small friendship network data we model throughout this paper. The FR layout is used. The teenagers' drinking behavior changes and the network becomes less densely connected over time. These are the mechanisms we hope to model with our chosen CTMCs.

easier to see and to make any changes in the network more noticeable. We visualize this data with a node-link diagram in Figure 2, where nodes are colored according to the girl's reported drinking behavior: does not drink, drinks once or twice a year, drinks once a month, and drinks once a week. We can see that, as time passes, the students seem to drink more and become increasingly isolated into smaller groups. An analysis of this type of data with a CTMC model should capture these dynamics in a way that allows the researcher to draw conclusions about the nature of the network and the behavioral forces at play.

Models: To our example data, we fit three different models. Each model uses a simple rate function, α_m, and an objective function with two or three parameters. Though our models are very simple, the model-vis techniques we present can easily be applied to much more complex models. The first model of interest, M1, contains the absolute minimum number of parameters in the objective function $f_i(x)$:

$$M1: \quad f_i(x) = \beta_1 s_{i1}(x) + \beta_2 s_{i2}(x), \tag{7}$$
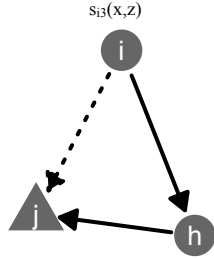
where $s_{i1}(x)$ is the density network statistic and $s_{i2}(x)$ is the reciprocity network statistic
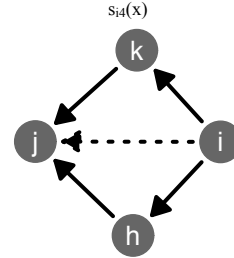
13
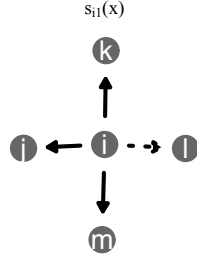
(a) Demonstrating the outdegree effect β_1. The dotted tie is encouraged if β_1 is positive. $s_{i1}(x) = \sum_j x_{ij}$
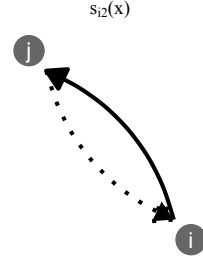
(b) Demonstrating the reciprocity effect β_2. The dotted tie is encouraged if β_2 is positive. $s_{i2}(x) = \sum_j x_{ij}x_{ji}$

(c) Demonstrating a JTT, where the covariate is represented by the shape of the nodes. The dotted tie is encouraged if β_3 is positive. $s_{i3}(x,z) = \sum_{j \neq h} x_{ij}x_{ih}x_{hj}\mathbb{I}(z_i = z_h \neq z_j)$

(d) Demonstracting a N22 between actors i and j. The dotted tie is encouraged if β_4 has a positive value. $s_{i4}(x) = |\{j : x_{ij} = 0, \sum_h x_{ih}x_{hj} \geq 2\}|$

Figure 3: The network statistics whose corresponding effects are included in the models we fit to the friends data.

for actor i at the current network state x (see Figure 3). The second and third models, M2 and M3, contain one additional parameter each in the objective function. We chose the additional parameters because they were significant (p-value < 0.05) according to a Wald-type test (`Wald.RSiena()`) provided in the `RSiena` software (Ripley et al., 2016). The model M2 contains an actor-level covariate parameter, and the model M3 contains an additional strutural effect in the objective function.

$$M2: \quad f_i(x, z) = \beta_1 s_{i1}(x) + \beta_2 s_{i2}(x) + \beta_3 s_{i3}(x, z) \tag{8}$$

$$M3: \quad f_i(x) = \beta_1 s_{i1}(x) + \beta_2 s_{i2}(x) + \beta_4 s_{i4}(x), \tag{9}$$

where $s_{i3}(x, z)$ and $s_{i4}(x)$ are defined in Figure 3. These statistics are known as the *number of jumping transitive triplets* (JTT) and the *number of doubly achieved distances two effect* (N22), respectively. The JTT effect emphasizes triads formed between actors with *different*

14

	M1	M2	M3
α_1	4.660 (0.059)	5.176 (0.068)	4.712 (0.060)
α_2	1.930 (0.026)	2.017 (0.028)	1.979 (0.027)
β_1	-3.597 (0.033)	-4.104 (0.038)	-3.589 (0.035)
β_2	4.149 (0.050)	4.277 (0.052)	4.230 (0.050)
β_3	–	3.209 (0.053)	–
β_4	–	–	-7.582 (1.746)

Table 1: The means (std. dev.) of parameter values estimated from 1,000 repeated fittings of M1, M2, and M3 to the example data.

covariate values, while the N22 effect emphasizes *indirect* ties between actors. All model effects are visualized in Figures 3a-3d, where the ties affected by the parameter value are represented by dotted lines. If the estimates of these parameters $\hat{\beta}_1, \ldots, \hat{\beta}_4$ are positive, the model encourages the tie represented by the dotted line to form, while the opposite is true if the parameter estimate is negative. Mean estimates from 1,000 repeated fittings are given in Table 1. Any time we simulate from a network model, these are the parameters we use.

We encourage interested readers to consult the `RSiena` manual for a complete definition and description of these and all other possible effects available to use in CTMC models (Ripley et al., 2017). Our goal here is to assess the fit of these models to our data, not to find the best model for this data, which is why we have kept both the data and the models very small. A true analysis of these data would include all of the available data, including additional covariates related to smoking and other behaviors, and would use sociological research to select and test the most pertinent effects at each step in the model hierarchy. The exact model structure and effects we choose are not as important to us as our ability to assess their impact on model fit. We keep the data and model simple in order to apply the more complicated model visualization tools that we discuss in Sections 3-5.

3   Model in the data space

Placing the model in the data space is crucial to understanding how well the model represents the observed data. We define the *data space* for our models as the combined data structures of the network: the node, edge, and time information. We use the `R` package `geomnet` to visualize the three data spaces together (Tyner and Hofmann, 2016). The package draws the network using node-link diagrams, and the network's node or edge data are then mapped to different visual features. The color, size, and shape of the points can be used to represent variables in the node data, while the color, linewidth, and linetype of the edges between nodes can be used to represent variables in the edge data. Finally, the networks observed at each time point are placed side-by-side, showing the network's evolution in time. Bringing all network information together in `geomnet` allows us to show the entire data space at once.

To view our models in the data space, we first simulate from the fitted model. No single network instance simulated from a CTMC will fully represent the model, so instead we look at an *expectation* from the network model. We frequently rely on expected values in statistics, but network models, especially those as complex as our CTMC models, lack an expected network measure. We could talk about expected values of parameters, but the parameters can be hard to interpret and do not illuminate the overall structure of the network. How then, can we arrive at an expected network? We propose the following method:

1. Condition on $x(t_1)$ and simulate 1,000 instances of $x(t_2)$ and $x(t_3)$ from the model of interest using previously estimated parameter values (see Table 1). Call these simulations $x^{(1)}(t_m), x^{(2)}(t_m), \ldots x^{(1000)}(t_m)$ for $m = 2, 3$.

2. Count the number of times each edge $i \to j$ appeared in one of the 1,000 network simulations. i.e. compute $x_{ij}^{(B)}(t_m) = \sum_{b=1}^{1000} x_{ij}^{(b)}(t_m)$ for $m = 2, 3$.

3. Construct one weighted summary network for time points 2 and 3. Each summary network has edge weights equal to the proportion of the simulated networks in which the edge appeared.i.e. $\bar{x}_{ij}(t_m) = x_{ij}^{(B)}(t_m)/1000$.
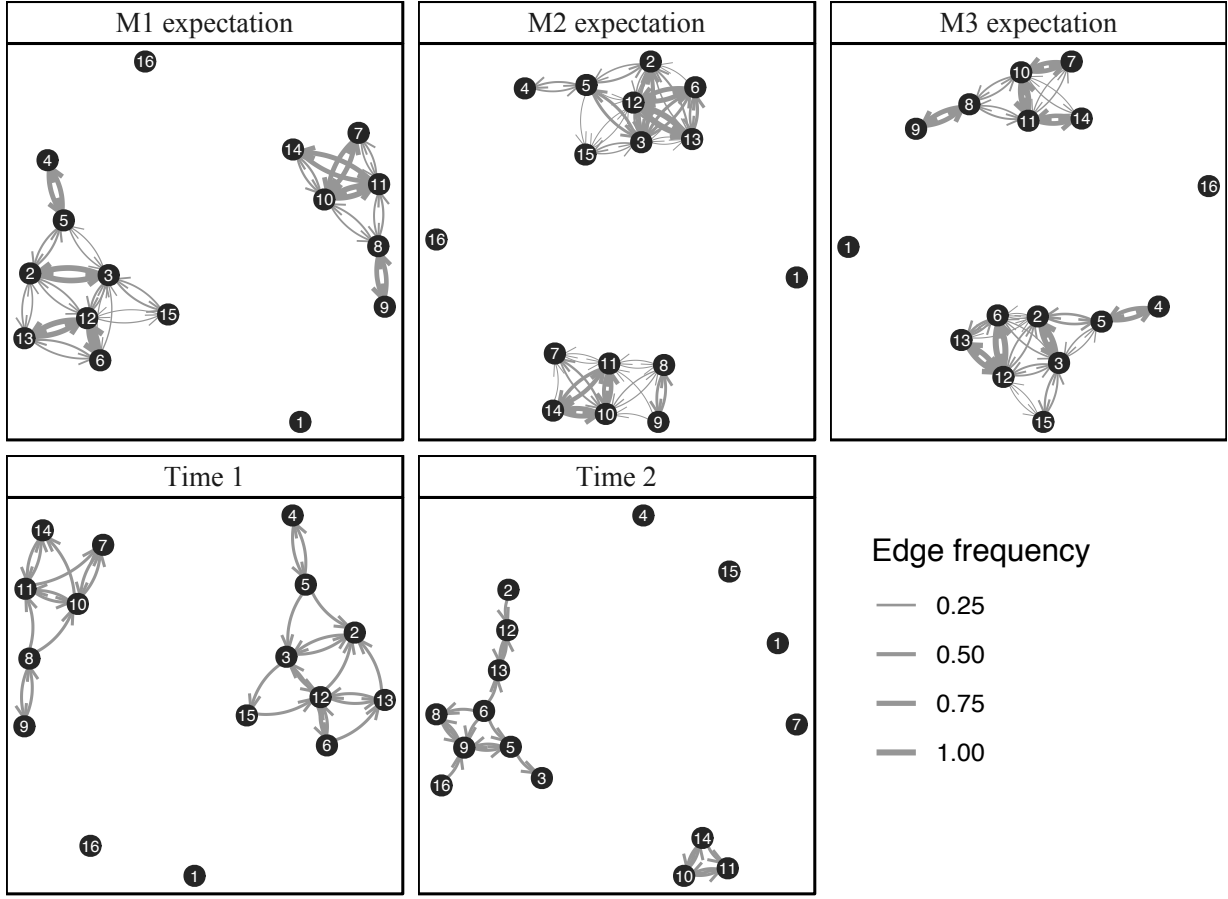
Figure 4: In the bottom left, the network at the first time point $(x(t_1))$, which is conditioned on in the model. In the bottom right, the network at the second time point $(x(t_2))$. In the top row, the three expected networks for time point 2 $(\bar{x}(t_2))$ according to model M1, M2, M3. Legend shows edge weights in the three expected networks.

4. Create the *expected network* by including only the edges that appeared in more than 5% of the simulations. i.e. $\bar{x}_{ij}(t_m) := \bar{x}_{ij}(t_m) \cdot \mathbb{I}(\bar{x}_{ij}(t_m) > 0.05)$. We write the expected networks as $\bar{x}(t_2)$ and $\bar{x}(t_3)$.

The above method can be generalized and applied to any network model, static or dynamic, from which we can simulate, for any number of simulations from the network. The expected networks from our three models of interest are shown in the top row of Figure 4. Edges that appear with higher frequency are drawn with thicker lines. On the bottom row of

Figure 4, we show the data for comparison: $x(t_1)$ on the left, and $x(t_2)$ on the right. Visualizing the expected network in this way places models M1, M2, and M3, in the data space, and helps assess model fit. For model M1 we can see that the overall structure of the average network is much more similar to $x(t_1)$ than to $x(t_2)$. In both $x(t_1)$ and $\bar{x}(t_2)$, there are two clusters of nodes: $\{2, 3, 4, 5, 6, 12, 13, 15\}$ and $\{7, 8, 9, 10, 11, 14\}$. The expected network, however, does not resemble $x(t_2)$, which it is supposed to represent. In $x(t_2)$, there is one small, strongly connected cluster and one larger, sparsely connected cluster, with four unconnected nodes. Because the expected network $x(\bar{t}_1)$ more closely resembles $x(t_1)$ than $x(t_2)$, we take this as evidence that the simple model, M1, is not a good fit to the data. Comparing the three expected networks to $x(t_1)$ and $x(t_2)$, we see that they all have nodes that are connected in the same groups as $x(t_1)$. Model M2, which included the transitive triplet parameter, results in more strongly connected components, as shown by the increased number of edges and the thicker lines between nodes. The lack of fit in all models is clear: not one of the three model expectations show node 16 gaining ties as it does in $x(t_2)$, nor do they show nodes 4 and 7 becoming isolated. In model M2, however, the ties to node 7 appear much weaker than in model M1 or model M3, and the nodes $\{10, 11, 14\}$ are also more strongly connected, as they are in wave 2 of data. This suggests that, despite the fact that neither of the three models is a good fit, M2 may be the best fitting model of the three. In a complete data analysis, we can use this information to select more models for analysis that utilize transitivity and covariate effects, as opposed to structural and indirect effects.

Another way to view our models in the data space is with *difference networks* between the expected network and the data, as shown in Figure 5. We created these networks by computing the difference between $\bar{x}(t_2)$ and $x(t_1)$, $\mathbf{A}(\bar{x}(t_2)) - \mathbf{A}(x(t_1))$, and the difference between $\bar{x}(t_2)$ and $\bar{x}(t_2)$, $\mathbf{A}(x(t_2)) - \mathbf{A}(\bar{x}(t_2))$ for model M1. The lack of model fit is also apparent in Figure 5, where the dashed edges represent ties that only show up in the expected network, and the solid edges representing ties in the data that the model fails to capture. Dotted edges are in both the expectation and the data and represent where the model is correct. On the left in Figure 5, we see the difference between $x(t_1)$ and the expected network. We see mostly dotted edges, meaning that the simulated networks
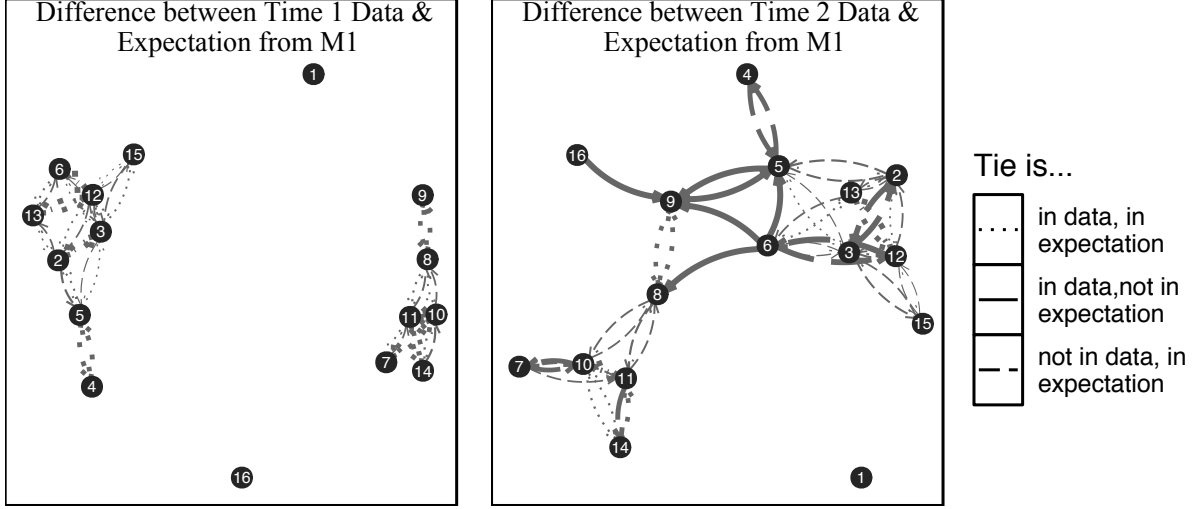
Figure 5: Differences between the expected network $\bar{x}(t_2)$ and $x(t_1)$ and $x(t_2)$. Some edges appear in both the data and the expected network $\bar{x}(t_2)$ (dotted lines), while others only appear in the data (solid lines) or only in the expectation (dashed lines). Width of non-data edges represent the proportion of appearances in the 1,000 simulations. The FR layout is used.

consist primarily of edges in $x(t_1)$, plus some new edges represented by the dashed lines that are not in the data. The unobserved ties are all reciprocating ties in the data, so the model is predicting more reciprocity between actors than there actually is. On the right in Figure 5, we see the difference between $x(t_2)$ and the expected network. Because the model is simulating $x(t_2)$, we would hope to see very few differences between the expected network and the data. However, there are six solid edges, which are in the data but do not appear at all in the expected network, and there are many dashed edges that appear in the expected network but are not in $x(t_2)$. Although there are some edges that appear in both the expected network and $x(t_2)$, the majority of edges in the expected network are not in the observed data, and there are several edges in the data missing from the expectation. We therefore conclude that the model M1 is a poor fit to our example data, which we have seen very clearly by viewing the model in the data space. As with the expected network, we can apply the difference network computation other network models to determine how closely the model fits the data.

4 Collections of models

Now that we have assessed model fit, we want to learn about model behavior in order to choose better fitting models in the future. To assess model behavior, we employ the second principle of model visualization: "collections are more informative" (Wickham et al., 2015). We rely on three methods for constructing collections of CTMC models. First, we explore the space of all possible models to determine significant model parameters. Second, we vary model settings to uncover relationships between parameters and their effects on the fitted model. Finally, we fit the model many times to assess the behavior of the underlying simulations. We chose these three collections because they each explore something different about model behavior: the choice of and relationships between parameters in the objective function and the stochastic effects from simulation.

Exploring the space of all possible models: The `RSiena` manual contains over 80 effects to include in the objective function (Ripley et al., 2017). To select objective function parameters for modeling our example data, we searched through all available parameters to find significant effects. The `RSiena` package includes the function `Wald.Rsiena` for Wald-type tests of parameter significance (Ripley et al., 2016). We start by including the outdegree and reciprocity parameters in the model then add one effect to the objective function, fit the model to the example data, test the added effect for significance, and repeat for all possible model parameters. Using this one-at-a-time testing method results in many possible significant parameters of different type and magnitude, demonstrating the flexibility of these models. We chose models M2 and M3 in addition to model M1 to examine more closely because their added effects had the smallest p-values from the Wald-type tests. This particular type of model exploration is applicable to any network model with an `R` package or other software that allows the user to identify model parameters, such as the `ergm` package, which has well over 100 effects for fitting exponential-family models to networks (Handcock et al., 2018; Hunter et al., 2008b).

Varying model settings: The second method for obtaining collections of models is to vary model settings. We have done this already by choosing three different models M1, M2, M3 to fit to our example data sets. CTMC models, however, are much more flexible than the three simple models we have chosen. Other models could have included different
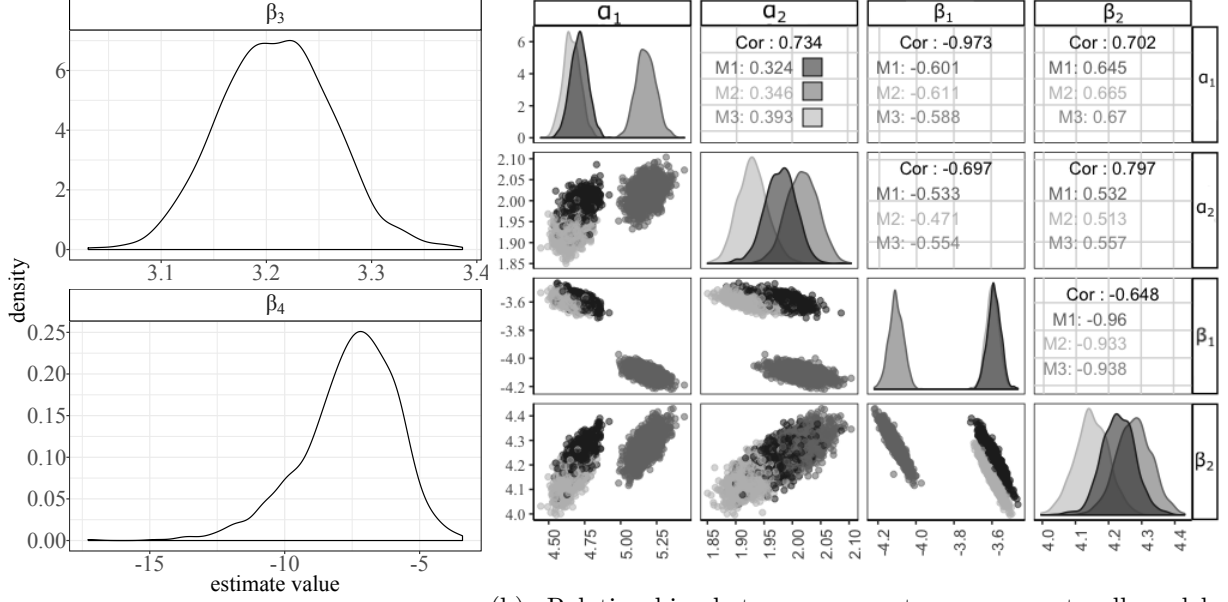
(a) Distribution of fitted β_3, β_4 values.

(b) Relationships between parameters common to all models. Densities and scatterplots are colored by model.

Figure 6: Distribution of fitted parameter values for our three models. The inclusion of β_3 or β_4 clearly has an effect on the distributions of the rate parameters, α_1 and α_2, and on the other objective function parameters β_1, β_2.

rate functions for each node, where for example the rate of change could depend on drinking behavior if we have reason to believe that girls who drink more change friends more frequently. We could also model the behavior changes, not just the network changes, if we believe that friends influence behavior via peer pressure. And as before, this method of gathering a collection of models can be used for any network model, such as the hierarchichal Bayesian network estimation model in the R package sna, which allows the user to vary hyperparameters in the prior and model parameters (Butts, 2016).

Fitting the model repeatedly: The simulations required to fit the CTMC network models lead to inherent variability in the fitted values. To examine this variability, we fit models M1, M2, and M3 to the friendship network 1,000 times each. The resulting means and standard deviations of the estimates are given in Table 1, and the distributions of all parameter estimates are shown in Figure 6. In Figure 6b, we can see that the addition of β_3 to the model results in very different estimates the of the other four parameters, α_1, α_2, β_1, and β_2. In fact, the distributions of α_1 and β_1 for M2 do not overlap at all with the

distribution of the same parameters from model M1. When β_3 is included, its estimate is postitive, meaning that friendships between two girls with different drinking behaviors tend to form when there is third girl who is already friends with the other two. The inclusion of β_3 also leads to increases in the estimates of α_1, α_2. Thus, when modeling the transitive triplet behavior in this way, the model concludes that girls change friends more frequently. It is not clear, however, that the addition of a parameter to the objective function should effect the estimates of the rate parameters.

On the other hand, the inclusion of the indirect tie parameter, β_4, does not lead to such drastically different estimates of other model parameters. The mean estimate of β_4 is large and negative, which suggests that indirect ties are strongly discouraged from forming. This is fairly intuitive given the context: teenage girls likely want to have direct friendships in tightly knit groups, so indirect relationships are not common. Finally, in Figure 6b, we demonstrate the relationship between each of pair of parameters common to all three models. The strongest correlation within each model is between β_1 and β_2, with absolute correlation greater than 0.90 in all three models. The β_1 parameter is also highly correlated with the β_3 parameter within model M2 (ρ = -0.755), but it is not as highly correlated with the β_4 parameter in model M3 (ρ = 0.419). The inherent relationship between effects is a known problem in network analysis (Goldenberg et al., 2010).

5   Explore algorithms, not just end result

The third and final model visualization principle, "explore the process of model fitting," is crucial to understanding the CTMC models (Wickham et al., 2015). When fitting models in `RSiena`, several simulation processes are hidden from the user. We refer to one of these hidden pieces in the SIENA MoM algorithm as the *microstep process*, which is a series of state changes in the CTMC as described in Section 1.2. At each microstep, an ego node is selected to change, and then randomly makes one change in its ties according to to the probabilities p_{ij} defined in Equation 5. The microstep process is a key piece of the model fitting procedure and is used in the third phase mentioned in Section 1.2.2 (Snijders, 2016). During modeling, the process proceeds until the network differs from the $x(t_m)$ by exactly C_m, as defined in Equation 3. Between two network observations $x(t_m)$ and $x(t_{m+1})$, there

can be dozens, hundreds, or even thousands of microsteps, depending on the size of the network and the value of C_m. We want to simulate and view these in-between steps in order to better understand the behavior of the CTMC model. The default in the software is discard the microsteps, which is practical and efficient if the goal is to fit a model to data, obtain parameter estimates, and draw conclusions or make predictions. But in order to understand how the models are fit, we need to extract and explore the different steps of the process, which is possible in `RSiena` with some small changes to the default settings. We use these steps to visually explore the algorithms, so that we are visualizing the model fitting process, and not only the model fitting result.
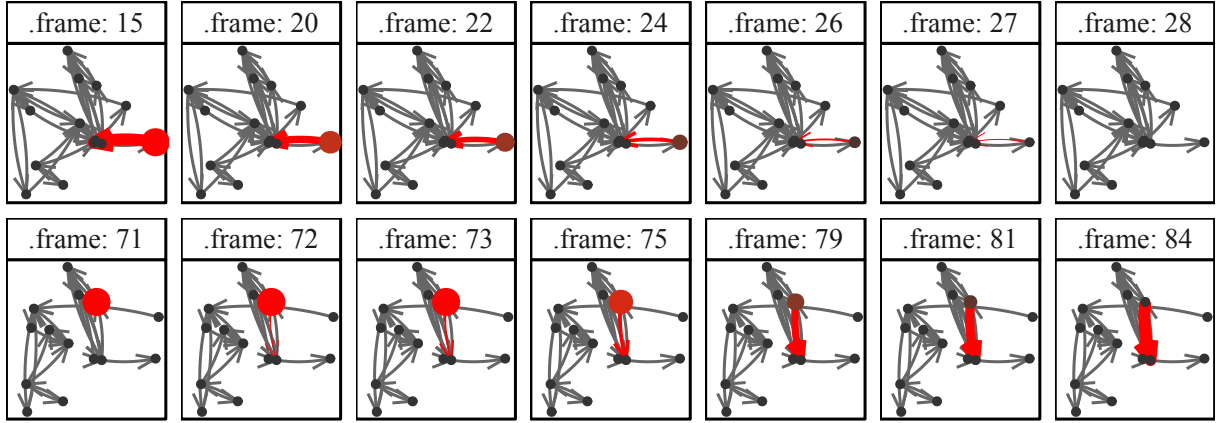

Figure 7: A selection of images in the microstep animation at `https://vimeo.com/240089108`. The selected edges and nodes are emphasized by changing size and color, then they fade in or out while the nodes change color and shrink to blend in with the other nodes. Frames 15-28 show edge destruction, while frames 71-84 show edge creation. A spring layout is used.

To visualize the underlying process, we animate the microsteps that form the CTMC from $x(t_1)$ to $x(t_2)$ for the example data. The microstep animation, some frames of which are shown in Figure 7, represents one possible path from $x(t_1)$ to $x(t_2)$ according to the model M1. We show each change in the network as follows: we first increase the size and change the color of the ego node to focus attention to its ties. Then, the changing tie either fades in or fades out. If there are no changes at a particular microstep, the microstep does not appear. Some frames of the animations are shown in Figure 7, and the full movie,

created with `tweenr` and `gganimate` can be viewed at `https://vimeo.com/240089108` (Pedersen, 2016; Robinson, 2016). Movies similar to this animation were used to visualize the changes of dynamic networks in Moody et al. (2005). Frames 15-28 of Figure 7 show a tie that is destroyed, while frames 71-84 show a tie that is created. For both changes, the ego node is emphasized with color and size. When a tie is removed, it is first emphasized with the same color and size as the node. As the animation proceeds, the tie shrinks and disappears as the ego node shrinks and changes color to match the others. If a tie is being added, it appears red from nothing, grows large for emphasis, then changes color and size to match the rest of the edges. In this network animation, we show the modeled steps of the unobserved CTMC process between two observed networks. We see each part of the hierarchical model: first, the selection of the ego node via the rate function, then the result of the actor maximizing its objective function by either deleting or adding a node. Finally, the layout of the network transitions as edges are removed or added, demonstrating how the overall network structure changes with each of the individual tie changes. Combining the tie changes in this animation makes the CTMC process the focus, demonstrating the underlying change mechanism of the dynamic network according to the model.

With this animation, we can see how the model behaves. Some tie changes appear to alter the overall network structure, as shown by the change in the layout of the nodes, while others seem to be inevitable, such as an added reciprocal tie between two nodes in a large connected group that do not change the layout. Other edges are created in one step and destroyed the next. When watching the animation, we are watching the model in action, which helps us better understand its behavior. This same animation method can be applied to any network model which changes one tie at a time. For example, the Erdös-Rényi random graph model is a series of tie additions, and we could animate the creation of a network from this model. Unlike CTMCs, however, Erdös-Rényi random graph models only create ties (Goldenberg et al., 2010). Regardless of the network model under consideration, animating the node-link diagram to view how the network changes gives insight into the model behavior and the process of model fitting.

We continue to use animation to view the changing structure of the network via adjacency matrix visualizations. In the first adjacency matrix visualization in Figure 8, we use
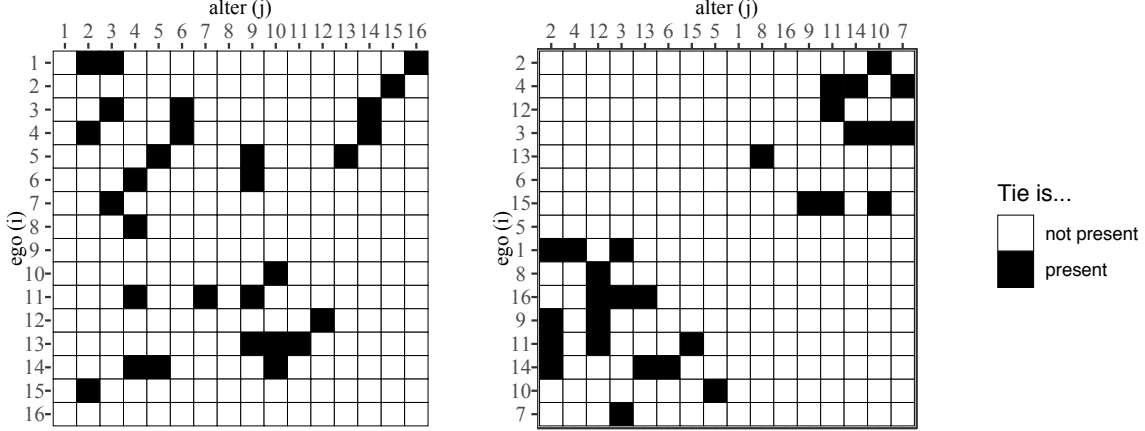
Figure 8: On the left, the first observation of the friendship network represented in adjacency matrix form, ordered by node ID. On the right, the same adjacency matrix is presented after seriation

the node ID to order the rows and columns. This arbitrary ordering does not easily convey the underlying structure of the network. We use *matrix seriation* to reorder the rows and columns of the adjacency matrix visualization so that the structure of the network is apparent (Liiv, 2010). To seriate the matrix, we first construct a cumulative adjaceny matrix, $\mathbf{A}^{cum}$, for the series of microsteps in the CTMC simulated from $x(t_m)$ to $x(t_{m+1})$. A single entry in the cumulative adjacency matrix, $\mathbf{A}_{ij}^{cum}$, is the total number of times the edge x_{ij} appears in the network from the initial observation, $x(t_m) \equiv X(0)$ to the last microstep, $X(R)$, where R is the total number of microsteps taken:

$$\mathbf{A}_{ij}^{cum} = \sum_{r=0}^{R} X_{ij}(r). \tag{10}$$

We then perform a principal component analysis (PCA) on $\mathbf{A}^{cum}$, and use the values of the first principal component to order the vertices on the x and y axes for the adjacency matrix net-vis. The resulting visualization for the first network observation is shown on the right in Figure 8. Using matrix seriation on the adjacency matrix visualization clearly shows the two distinct connected components in the first network, which are difficult to find in the visualization ordered by node ID. We continue to use the seriated matrix in another animation of the microstep process, which is available at `https://vimeo.com/240092677`. Some frames of the video are shown in Figure 9. In the animation, a square appears or

25

disappears when the edge it represents appears or disappears in the microstep process. This animation, unlike the previous one, shows the microsteps where the chosen node does not make a change. Starting at frame 0 (the first network observation $x(t_1)$), there are two clearly connected components: one in the bottom left, and one in the top right. With each frame, we see the network evolve: sometimes ties are removed right after they are created, and sometimes several ties are removed or created in a row. By the end, the bottom left component has become more sparsely connected, while the top right component has shrunk, but remains closely connected. In contrast to the node-link animation, the adjacency matrix animation shows how the algorithm explore the space of all possible networks, because possible edges are represented in each frame of the adjacency matrix animation. It is also easier to see the connected components of the graph in this animation because we have clearly grouped them with matrix seriation. As with the node-link animation, the adjacency matrix animation could also be used for other dynamic network models. Because the adjacency matrix emphasizes edges, this animation method is best for large directed networks whose structure is easier to see in an adjacency matrix visualization than in a node-link visualization (Ghoniem et al., 2005). Both animation methods demonstrate model behavior that would have not been seen with traditional visualizations or computations.

6 Discussion

We have used several visualization methods, some old and some new, to diagnose and understand network models in new ways. Though we have applied these methods to CTMC models for dynamic social networks, all of our visualizations can be applied to other dynamic network models and most can also be applied to any static network model. We gained insight into and appreciation for complicated and flexible network models by following the guiding principles of model visualization: viewing the model in the data space, visualizing collections of models, and looking at the underlying algorithms (Wickham et al., 2015). When we look at the model in the data space by viewing the expected network simulated from a model, we are able to easily see the lack of model fit. Computing and visualizing the difference network between the data and the expected network also helps assess model fit
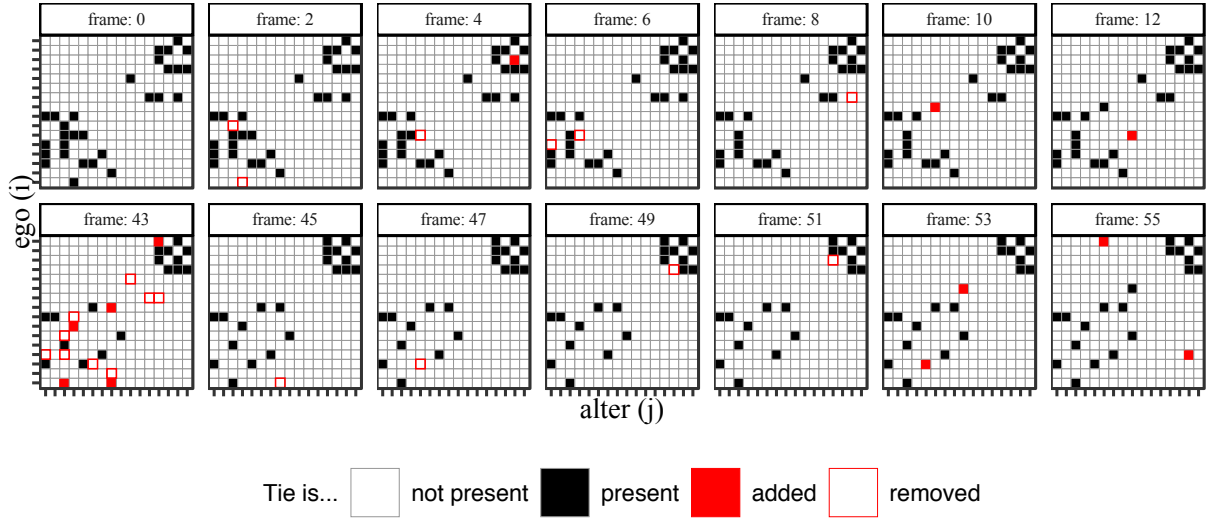
Figure 9: A selection of frames from the adjacency matrix visualization animation for one series of microsteps. The node labels are removed to declutter the figure. Complete video available at https://vimeo.com/240092677.

by showing us where the model is completely missing the data. When exploring collections of models, we learn more about the large number of parameters possible in network models, and we can also uncover relationships between these parameters. Finally, when we explore the algorithms fitting the models, we have a better understanding of the model and its stochastic behavior. All in all, this three-pronged model-vis attack has uncovered many properties of CTMC models for social networks and shows great potential for application to other network models.

We have only just begun to scratch the surface of these multi-layered models for social networks. The RSiena software is incredibly powerful, and we can fit much more flexible hierarchical models than we have examined here. If, for example, we think the network structure or an actor covariate affects the rate of change of the network, we can incorporate that belief into the rate function. In addition, more than one actor-level covariate can be included in the model, and many more than three parameters can be included in the objective function. As we have shown, the rate and objective function parameters are often highly correlated, so researchers can now use model-vis techniques to gain a better

understanding of these correlations and hopefully find ways to account for their effects in the model. In addition, some extensions of the CTMC model can aslo model behavior change of the actors in the network, which we have just treated as covariates. The CTMC family of models for dynamic networks has immense potential for additional model visualization applications.

Furthermore, the data we have used are quite small by network data standards, with only 16 nodes. Thus, some of the visualizations we have presented, such as the small node-link diagram animation, may not scale up to larger networks. Future network model-vis research could also include interactive and/or three-dimensional graphics, which we did not explore here. Interactivity is the state-of-the-art in data visualization, and network visualization is just starting to catch on (see e.g. Kairam et al., 2015). Wickham et al. (2015) also relied on interactive tools like GGobi (Swayne et al., 2003) for interactivity, and for networks, there is some interactive support with the package `plotly` built into `geomnet` (Sievert et al., 2017; Tyner and Hofmann, 2016).

We hope that the principles of model-vis continue to be used for learning more about the fit and behavior of statistical models for network data. Our model-vis application has uncovered many properties of CTMC models for dynamic social networks, and potential abounds for application of model-vis in other areas of network analysis.

Online supplemental material:

Much of the code used to create the visualizations in this paper has been packaged and made available online at `https://github.com/sctyner/netvizinf` and `https://github.com/sctyner/geomnet` (also on CRAN). Additional, non-packaged code can be found at `http://bit.ly/ctmc-model-viz`.

References

Butts, C. T. (2016), *sna: Tools for Social Network Analysis*, R package version 2.4.

Chyzh, O. (2016), "Dangerous liaisons: An endogenous model of international trade and human rights," *Journal of Peace Research*, 53, 409–423.

Fekete, J.-D. (2009), "Visualizing Networks using Adjacency Matrices: Progresses and Challenges," in *11th IEEE International Conference on Computer-Aided Design and Computer Graphics*, pp. 636–638.

Frank, O. and Strauss, D. (1986), "Markov Graphs," *Journal of the American Statistical Association*, 832–842.

Fruchterman, T. M. and Reingold, E. M. (1991), "Graph Drawing by Force-Directed Placement," *Software: Practice and Experience*, 21, 1129–1164.

Ghoniem, M., Fekete, J.-D., and Castagliola, P. (2005), "On the readability of graphs using node-link and matrix-based representations: a controlled experiment and statistical analysis," *Information Visualization*, 4, 114.

Gibson, H., Faith, J., and Vickers, P. (2013), "A survey of two-dimensional graph layout techniques for information visualisation," *Information Visualization*, 12, 324–357.

Goldenberg, A., Zheng, A. X., Fienberg, S. E., and Airoldi, E. M. (2010), "A Survey of Statistical Network Models," *Foundations and Trends in Machine Learning*, 2, 129–233.

Handcock, M. S., Hunter, D. R., Butts, C. T., Goodreau, S. M., Krivitsky, P. N., and Morris, M. (2018), *ergm: Fit, Simulate and Diagnose Exponential-Family Models for Networks*, The Statnet Project (`http://www.statnet.org`), R package version 3.9.4.

Hoff, P. D., Raftery, A. E., and Handcock, M. S. (2002), "Latent Space Approaches to Social Network Analysis," *Journal of the American Statistical Association*, 97, 1090–98.

Holland, P. W. and Leinhardt, S. (1977), "A dynamic model for social networks," *The Journal of Mathematical Sociology*, 5, 5–20.

Hunter, D. R., Goodreau, S. M., and Handcock, M. S. (2008a), "Goodness of fit of social network models," *Journal of the American Statistical Association*, 103, 248–258.

Hunter, D. R., Handcock, M. S., Butts, C. T., Goodreau, S. M., and Morris, M. (2008b), "ergm: A Package to Fit, Simulate and Diagnose Exponential-Family Models for Networks," *Journal of Statistical Software*, 24, 1–29.

Kairam, S., Riche, N. H., Drucker, S., Fernandez, R., and Heer, J. (2015), "Refinery: Visual Exploration of Large, Heterogeneous Networks through Associative Browsing," *Computer Graphics Forum (Proc. EuroVis)*, 34.

Kamada, T. and Kawai, S. (1989), "An Algorithm for Drawing General Undirected Graphs," *Information Processing Letters*, 31, 7–15.

Knuth, D. E. (2013), *Combinatorics: Ancient and Modern*, Oxford University Press, chap. Two thousand years of combinatorics.

Liiv, I. (2010), "Seriation and Matrix Reordering Methods: An Historical Overview," *Statistical Analysis and Data Mining*, 3, 70–91.

Michell, L. and Amos, A. (1997), "Girls, pecking order and smoking," *Social Science & Medicine*, 44, 1861–1869.

Moody, J., McFarland, D., and Bender-deMoll, S. (2005), "Dynamic Network Visualization," *American Journal of Sociology*, 110, 1206–1241.

Pedersen, T. L. (2016), *tweenr: Interpolate Data for Smooth Animations*, R package version 0.1.5.

R Core Team (2016), *R: A Language and Environment for Statistical Computing*, R Foundation for Statistical Computing, Vienna, Austria.

Ripley, R., Boitmanis, K., Snijders, T. A., and Schoenenberger, F. (2016), *RSiena: Siena - Simulation Investigation for Empirical Network Analysis*, R package version 1.1-304/r304.

Ripley, R. M., Snijders, T. A., Boda, Z., Vörös, A., and Preciado, P. (2017), *Manual for RSiena*, University of Oxford: Department of Statistics; Nuffield College; University of Groningen: Department of Sociology, `https://www.stats.ox.ac.uk/~snijders/siena/RSiena_Manual.pdf`.

Robbins, H. and Monro, S. (1951), "A stochastic approximation method," *The Annals of Mathematical Statistics*, 22, 400–407.

Robinson, D. (2016), *gganimate: Create easy animations with ggplot2*, R package version 0.1.0.9000.

Schaefer, D. R., Kornienko, O., and Fox, A. M. (2011), "Misery Does Not Love Company: Network Selection Mechanisms and Depression Homophily," *American Sociological Review*, 76, 764–785.

Schloerke, B., Crowley, J., Cook, D., Hofmann, H., Wickham, H., Briatte, F., Marbach, M., and Thoen, E. (2016), *GGally: Extension to ggplot2.*, R package version 1.3.0.

Schweinberger, M. (2012), "Statistical modelling of network panel data: Goodness of fit," *British Journal of Mathematical and Statistical Psychology*, 65, 263–281.

Sievert, C., Parmer, C., Hocking, T., Chamberlain, S., Ram, K., Corvellec, M., and Despouy, P. (2017), *plotly: Create Interactive Web Graphics via 'plotly.js'*, R package version 4.7.1.

Snijders, T. A. (2016), *Siena Algorithms*, University of Oxford: Department of Statistics, `https://www.stats.ox.ac.uk/~snijders/siena/Siena_algorithms.pdf`.

Snijders, T. A., van de Bunt, G. G., and Steglich, C. E. (2010a), "Introduction to stochastic actor-based models for network dynamics," *Social Networks*, 32, 44 – 60.

Snijders, T. A. B. (1996), "Stochastic actor-oriented models for network change," *Journal of Mathematical Sociology*, 21, 149–172.

— (2001), "The Statistical Evaluation of Social Network Dynamics," *Sociological Methodology*, 31, 361–395.

— (2017), "Stochastic Actor-Oriented Models for Network Dynamics," *Annual Review of Statistics and Its Application*, 4, 346–363.

Snijders, T. A. B., Koskinen, J., and Schweinberger, M. (2010b), "Maximum Likelihood Estimation for Social Network Dynamics," *The Annals of Applied Statistics*, 4, 567–588.

Swayne, D., Temple Lang, D., Buja, A., and Cook, D. (2003), "GGobi: Evolving from XGobi into an Extensible Framework for Interactive Data Visualization," *Computational Statistics & Data Analysis*, 43, 423–444, see also `http://www.ggobi.org`.

Tamassia, R. (ed.) (2013), *Handbook of Graph Drawing and Visualization*, CRC Press.

Tyner, S. and Hofmann, H. (2016), *geomnet: Network Visualization in the 'ggplot2' Framework*, R package version 0.2.0.9001.

Watts, D. J. and Strogatz, S. H. (1998), "Collective dynamics of 'small-world' networks," *Nature*, 393, 440.

Wickham, H. (2009), *ggplot2: Elegant Graphics for Data Analysis*, useR, Springer.

Wickham, H., Cook, D., and Hofmann, H. (2015), "Visualizing statistical models: Removing the blindfold," *Statistical Analysis and Data Mining: The ASA Data Science Journal*, 8, 203–225.

Yin, G. G. and Zhang, Q. (2010), *Continuous-Time Markov Chains and Applications: A Two-Time-Scale Approach*, New York: Springer, 2nd ed.